

Producing low fluorine mold powder by replacing CaF_2 with Na_2CO_3 , ZnO and Fe_2O_3

A.R. Arefpour^{1*}, A. Monshi², A. Saidi³ and T. Khayamian⁴

Department of Materials Engineering, Najaf Abad Branch, Islamic Azad University, Esfahan, Iran

Abstract

Mold powders in continuous casting of steel contain fluorine through mainly CaF_2 and occasionally NaF and Na_3AlF_6 . Fluorine develops dangerous gases such as SiF_4 and HF at high temperatures. In this study, CaF_2 is partly replaced by substances such as Na_2CO_3 , ZnO and Fe_2O_3 . Sulfur free Portland cement clinker containing gypsum was used as a new product base. These additions developed comparable viscosity to the industrially used powder. In order to compare the viscosity of laboratory samples with the reference sample, study the crystalline behavior of samples, and compare them to the reference sample, there were performed sloped plate groove viscometer, XRD and SEM studies. It can be detected the Crystalline phases such as Gehlenite, Nepheline, Akermanite, Cuspidine, $\text{Na}_2\text{ZnSiO}_4$, $\text{Ca}_2\text{ZnSi}_2\text{O}_7$, Ca_3SiO_5 and Mn_3O_4 , Fe_2SiO_4 . In order to develop less toxic mold powder in continuous casting of steels, it is proposed being crystalline and glassy with comparable viscosity.

Keywords: Mold powder, Viscosity, Crystalline Behavior.

1. Introduction

Continuous casting is one of the most important operational units in the general process of steel production to improve yield and steel quality¹⁾. More than 90 % of the steel in the world is produced in this way²⁾. Mold powders play an important role in the stability of the continuous casting process in all casting speeds. The main duty of mold slag, in other words the molten powder, is to provide adequate lubrication and heat transfer control horizontally between the steel crust and copper mold^{3,4)}.

The other duties of mold powder are to protect molten steel from oxidation, insulate molten steel against heat loss, absorb impurities from molten steel, adjust mold wall heat transfer, and minimize the formation of surface defects^{5,6)}. The Mold powder is a thin slag layer between the mold and steel crust usually including molten, crystalline and glass layers. The Heat transfer from the steel crust to the mold has been through conductivity and radiation heat through slag layers and heat resistance at the slag- mold interface⁷⁾. Mold powders are usually composed of substances such as Al_2O_3 , MgO , Na_2O , SiO_2 , CaO beside fluorine. The fluorine's duty is viscosity control, solidification temperature, and to improvement of the crystalline fraction in the slag film⁸⁻¹⁰⁾.

Fluorine can be added to the mold powder composition as CaF_2 ¹¹⁾. Cuspidine ($3\text{CaO} \cdot 2\text{SiO}_2 \cdot \text{CaF}_2$) has generally been recognized as the main crystalline phase in the

lubricant film^{12,13)}. The emission of Fluorine is a cause for the corrosion of plant equipment, acidity of water refrigerant, and endangerment of the safety and the health⁸⁾. Almost all powders containing CaF_2 reduce the viscosity and the melting point of lubricants¹⁴⁾. Slag viscosity is a function of slag composition and the structure related to alkalinity selection being one of its limitations¹⁵⁾.

In This study has been used iron and zinc oxide as well as sodium carbonate to decrease or substitute fluorine in mold powder composition. The viscosities of prepared powders were compared with the reference sample, and XRD, SEM were performed to compare the crystalline behavior of these powders with the reference sample.

2. Materials and Research Method

2.1 Samples Preparation

The industrial granulated powder used in the high speed continuous casting of steel at Mobarakeh Steel Complex of Esfahan is called granulated mold powder (original powder). The chemical composition of this powder which based on weight percentage is given in Table 1.

The minerals used to prepare the laboratory samples in this study include silica (SiO_2), manganese oxide (MnO), magnesium oxide (MgO), sodium carbonate (Na_2CO_3), iron oxide (Fe_2O_3), zinc oxide (ZnO) and fluorine (CaF_2) together with portland cement clinker with its chemical analysis based on weight percentage according to Table 2. In This study, it has been used portland cement clinker as the main component to make laboratory samples because of its close similarity to the composition of the original powder. Moreover, the prepared samples had to be free from harmful sulfated compounds, so portland cement clinker had

* Corresponding author:

Tel: +98 (913) 1019125,

Fax: +98 (311) 2350352

Email: arefpr.arz@gmail.com

Address: Department of Materials Engineering, Najaf Abad Branch, Islamic Azad University, Esfahan, Iran.

1. M.Sc.

2,3,4. Professor

this qualification. Thus, three 50- gram samples were prepared with different chemical compositions based on weight percentage according to Table 3. It should be noted that the chemical analysis of samples has been determined based on 100%wt ignoring heat loss. In order to homogenizing the powders, the mechanical grinding was used. Thus, the powders with defined weights along with ethanol 96% purity and similar weight as the powders were placed in the slots of a ball grinder and mixed for 150 seconds with a speed of 600 rpm. Then, the ground powders were dried in an oven at 110 °C for three hours. After drying the powders, 1 gram of each powders was pressed with the original powder at the pressure of 3 MPa by a press machine. The size of obtained samples was 13 mm in diameter and 2 mm in height. Then, these samples were placed on the viscometer.

Table 1. The Composition of the original powder based on weight percent.

Chemical composition	Weight percent
LOI	15- 18
C _(total)	7-9
C _(free)	4.5 – 6.5
SiO ₂	28 – 29.5
Fe ₂ O ₃	1 – 2.5
Al ₂ O ₃	3 – 5
CaO	26 – 28
MgO	5 – 6
Na ₂ O + K ₂ O	6 – 8
MnO	4 – 6
Fluorine (F ⁻)	3 – 4
S	< 0.3
H ₂ O (120 °C)	< 0.8

Table 2. The Chemical analysis of Portland cement clinker in terms of weight percent.

Chemical Composition	Weight percent
SiO ₂	21.78
Al ₂ O ₃	5.41
Fe ₂ O ₃	3.14
CaO	64.32
MgO	1.89
K ₂ O	0.73
Na ₂ O	0.28
SO ₃	0.01

Table 3. The Chemical analysis of prepared samples based on weight percent.

sample	CaO	SiO ₂	Al ₂ O ₃	Fe ₂ O ₃	MnO	MgO	Na ₂ O	K ₂ O	F ⁻	ZnO	C	S
A	34.81	32.18	2.54	4.56	6.13	5.75	8.89	0.34	3.09		1.69	0.004
B	35.54	32.86	2.6	1.5	6.26	5.87	9.08	0.35	3.16	1.05	1.72	0.004
C	35.65	32.96	2.61	1.51	6.28	5.89	9.72	0.35	3.17		1.86	0.004

2.2 Viscosity Comparison

A groove viscometer disk was used to compare viscosities. The pressed samples were placed on the top part of the groove viscometer and the viscometer was placed on a surface by 45° slope. The set of the viscometer and samples was then put inside a furnace. In order to prevent cracking or breaking the viscometer and ruining the pressed samples, the furnace was first heated to 400 °C for 30 minutes. Thereafter, the temperature of furnace was increased to 1150 °C. At this temperature, the samples melted. Finally, the samples cooled off outside of the furnace. At 1150 °C, it was possible to compare viscosities and the lubrication of prepared samples with the reference sample.

3. Results and Discussion

3.1 Viscosity

The original powder which was melted on the groove viscometer at 1150 °C was considered as the reference sample, so that the difference between viscosities and crystalline behaviors of laboratory samples were compared with the reference sample.

After cooling off the set inside the furnace and removing the viscometer from the furnace, molten samples on the viscometer were studied (Fig.1). In the sample A which it was added 4.56wt% Fe₂O₃ and 3.09wt% F⁻, it was observed that a viscosity similar to the reference sample was attained. In other words, the substitution of hematite inside of flour indicates a suitable performance by hematite in the mold powder. It can be concluded that hematite helps to fluorine to control mold powder viscosity. Also, a little amounts of Fe₂O₃ beside fluorine has led to decrease in mold powder viscosity. It seems that hematite acts similarly to fluorine in the chemical composition of continuous casting mold powder. It can bring about controlled viscosity and desirable lubrication. The use of 1.05wt% ZnO and 3.16wt% F⁻ in the sample B showed that ZnO has a suitable performance similar to hematite in the mold powder and consequently, it was attained a viscosity similar to the reference sample. It seems that Zinc oxide along with fluorine can be a suitable low-fluorine sample as a favorable lubricant use in continuous casting of steel industry. In the sample C, the amount of fluorine was decreased and sodium carbonate was used as a source of sodium oxide as a lubricant. It was observed in this sample that when fluorine is decreased, F⁻ and sodium oxide are increased to 3.17wt% and 9.72wt% in the mold powder composition, respectively. The composition of sample C includes 3.17wt% F⁻ which it has been replaced

instead of fluor. The amount of Na_2O has increased from 8.63wt% to 9.72wt%. Increasing 1.09wt% Na_2O leads to attain a suitable lubricant with a comparable viscosity relative to the reference sample. Na_2O is a lubricating oxide. If it is associated with fluorine in the chemical composition of continuous casting mold powder, then it can be considered as a suitable low-fluorine substitution for the main mold powder used in continuous casting of steel industry.

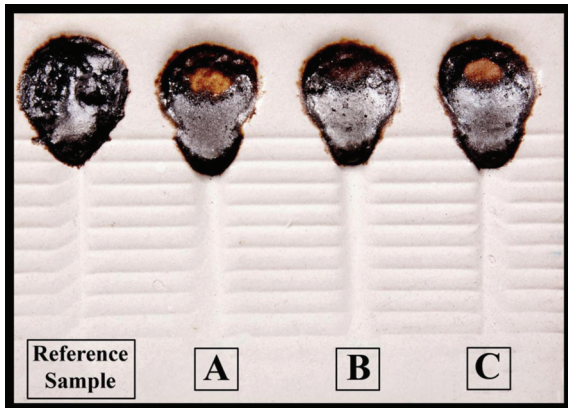


Fig. 1. Schematic illustration of molten samples on the groove viscometer.

3.2. Crystalline Behavior

In order to identify the original powder and to compare the crystalline behavior of the prepared samples to that of the reference sample, there were performed XRD, SEM analyses on the molten samples on the viscometer.

The XRD analysis of the original powder showed that wollastonite (CaSiO_3), Silica (SiO_2), hematite (Fe_2O_3), corundum (Al_2O_3), manganese silicate (MnSiO_3), sodium carbonate (Na_2CO_3), $\text{CaMg}(\text{SiO}_3)_2$ and CaAl_2O_4 are the predominant phases in the XRD analysis of this sample (Fig. 2).

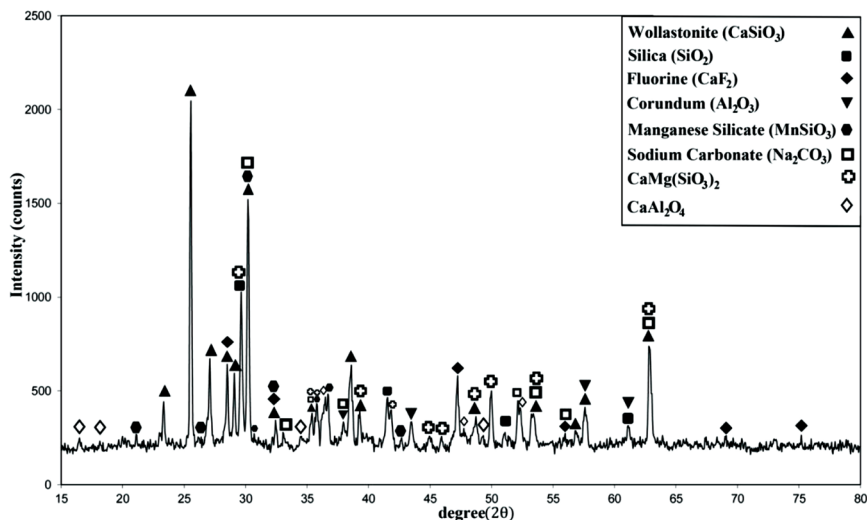


Fig. 2. The Schematic illustration of XRD analysis of the original powder.

In the SEM images of original powder at 3000x and 9000x (Fig.3(a) and 3(b)), it has been shown the morphology of the original powder.

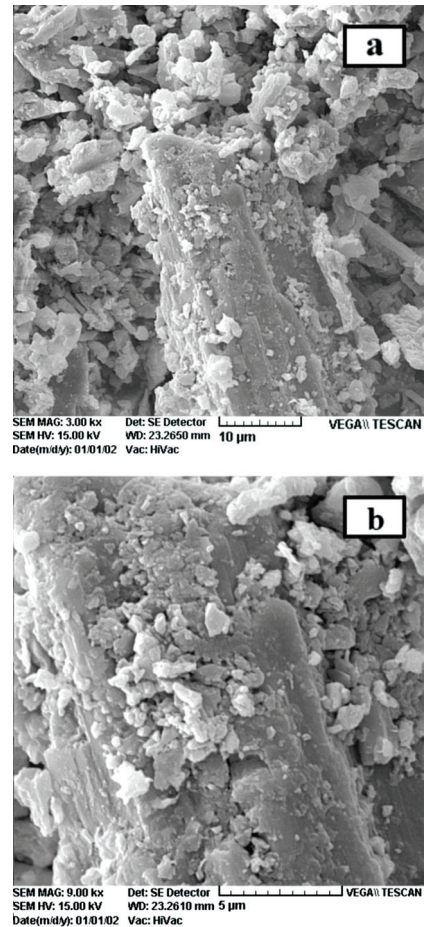


Fig. 3. SEM images of the original powder: (a) 3000x and (b) 9000x.

The granulated industrial powder which was used as the original powder was fired and melted at a high temperature in the furnace. It was observed gehlenite

($\text{Ca}_2\text{Al}_2\text{SiO}_7$), cuspidine ($\text{Ca}_4\text{F}_2\text{Si}_2\text{O}_7$), akermanite ($\text{Ca}_2\text{MgSi}_2\text{O}_7$) phases. These phases have the main peak in the highest possible intensity in the XRD pattern of the reference sample. Also, it was detected nepheline ($\text{NaAlSi}_3\text{O}_8$) and M_3O_4 phases in the XRD of this sample (Fig.4).

The SEM images of the reference sample at 3000x and 9000x (Figs.5(a) and (b)) showed the presence of crystals in the extended molten background which is the result of glass formation. Several formed silicates

are detectable in the XRD analysis which the formation of these silicates is due to being saturated the glass by silica during cooling off. They are useful for mold powder. Because Silicate crystals in the glass matrix control the horizontal heat transfer, they prevent from the very low viscosity which can occur at the melting point of steel, i.e. 1600 °C, leading to an abrupt fall of extraordinary melt of the fluid. Therefore, these silicates provide desirable viscosity to establish a suitable condition to cool off the ingot.

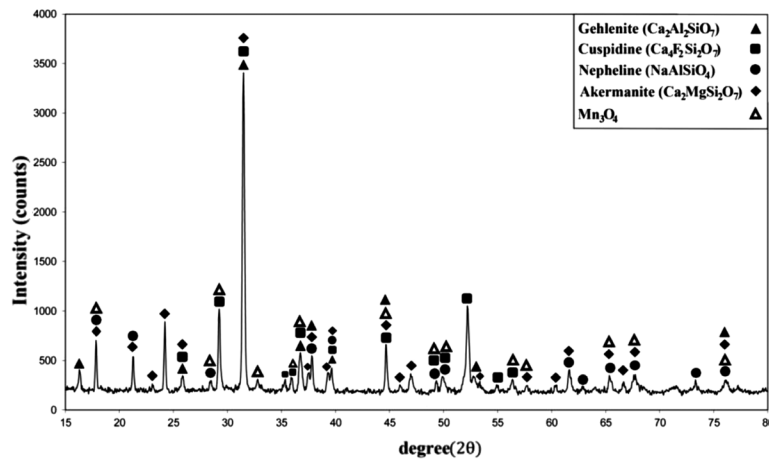


Fig. 4. The Schematic illustration of XRD analysis of the molten reference sample.

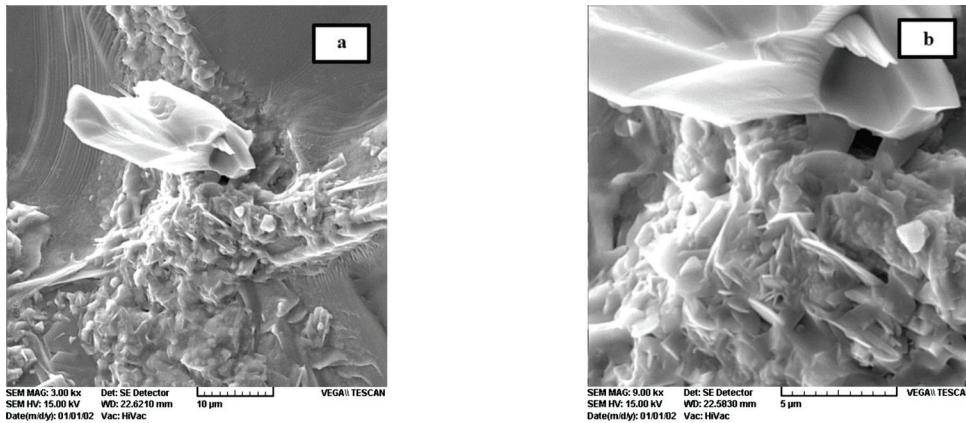


Fig. 5. SEM images of the molten reference sample: (a) 3000x and (b) 9000x.

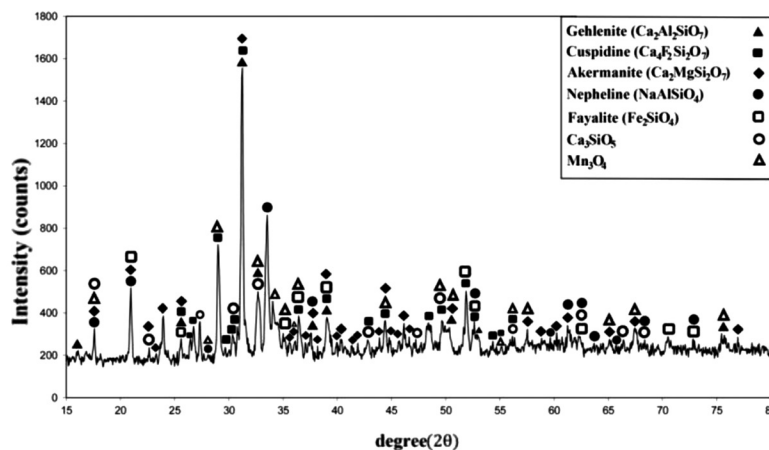


Fig. 6. The Schematic illustration of XRD analysis of the sample A.

Increasing in hematite and decreasing in fluorine in the sample A, the XRD analysis showed the phases of gehlenite, cuspidine, akermanite, fayalite (Fe_2SiO_4) beside phases such as Ca_3SiO_5 , Mn_3O_4 and nepheline (Fig.6). It seems in this sample that the phases of gehlenite, cuspidine, akermanite and the new phase of fayalite have led to the formation of crystalline deposits and control mold powder viscosity in optimized casting conditions. SEM images of this sample (Figs.7(a) and (b)) at 3000x and 9000x show that it seems to be a mixture of crystals developed inside the glass; as a result, it leads to decrease in mold powder viscosity.

In the sample B, it was observed that adding Zinc oxide and large amount of sodium oxide to cuspidine, gehlenite, and akermanite lead to the formation of $\text{Na}_2\text{ZnSiO}_4$ and Ca_2SiO_7 phase. Moreover there are detectable phases such as Ca_3SiO_5 and Mn_3O_4 in Fig. 8 which shows the XRD analysis of the sample C. It seems that adding ZnO to this sample lead to the control of mold powder viscosity due to developing

phases such as $\text{Na}_2\text{ZnSiO}_4$ and $\text{Ca}_2\text{ZnSi}_2\text{O}_7$, along with phases such as gehlenite and cuspidine.

Considering SEM images at 3000x and 9000x (Figs.9(a) and (b)), it can be seen a mixture of Crystals in the glass background.

In sample C, it was detected the nepheline phase with increase in Na_2CO_3 . Also, there were observed phases such as cuspidine, gehlenite, akermanite along with Ca_3SiO_5 and Mn_3O_4 (Fig.10). The XRD analysis of this sample was very similar to XRD analysis of the reference sample. It means that Na_2CO_3 can replace CaF_2 in industrial operations.

SEM images of the sample C at 3000x and 9000x (Figs.11(a) and (b)) show that a cavity has been formed due to the release of CO_2 in the high viscose melt but not refilled by the melt. In other words, SEM images of the Sample C showed the existence of various crystals in the glass matrix. It is resulted that these crystals in the glass matrix perform viscosity control of the sample C similar to crystals which control the viscosity of the reference sample (Fig. 5).

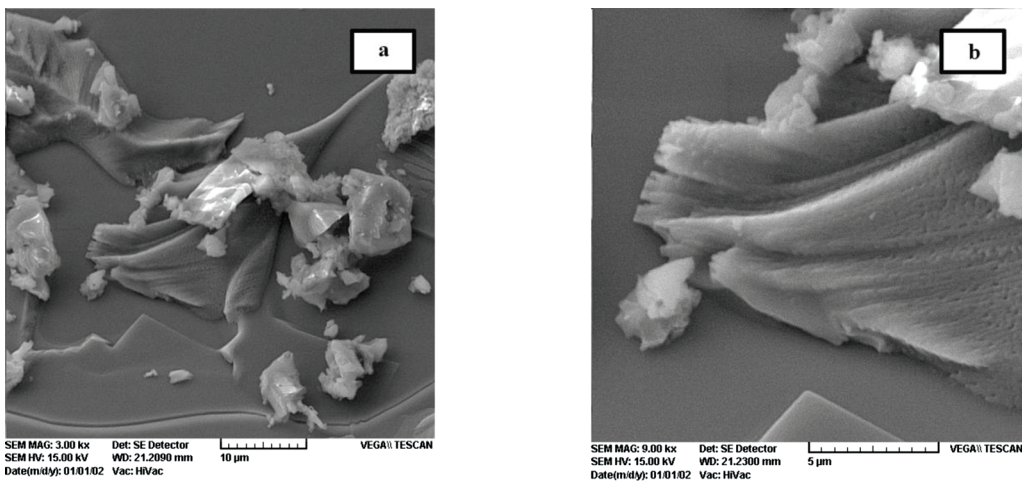


Fig. 7. SEM images of the sample A: (a) 3000x and (b) 9000x.

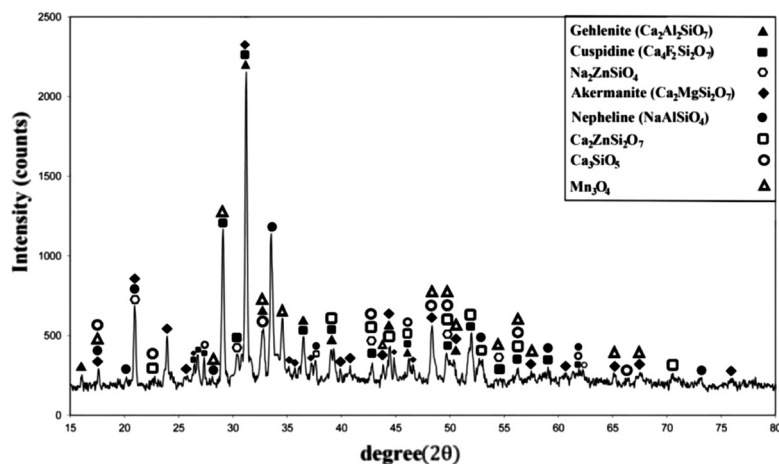


Fig. 8. XRD analysis of the sample B.

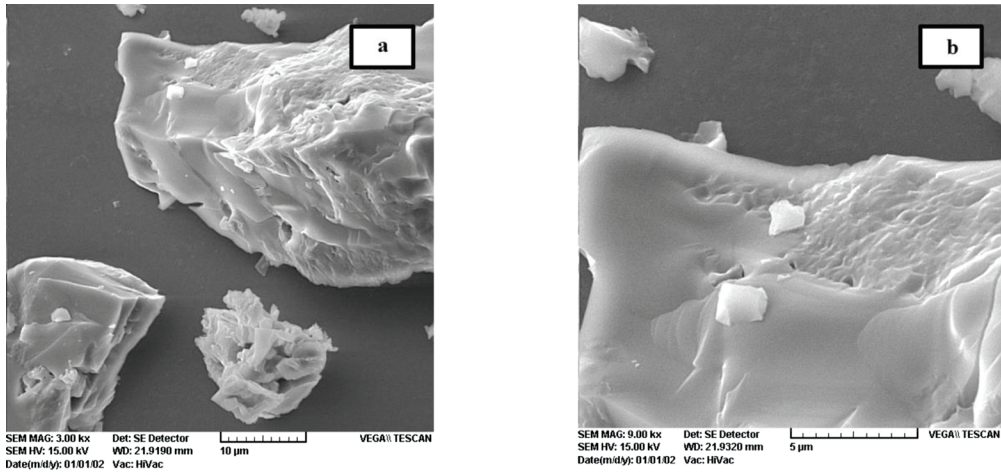


Fig. 9. SEM images of the sample B: (a) 3000x and (b) 9000x.

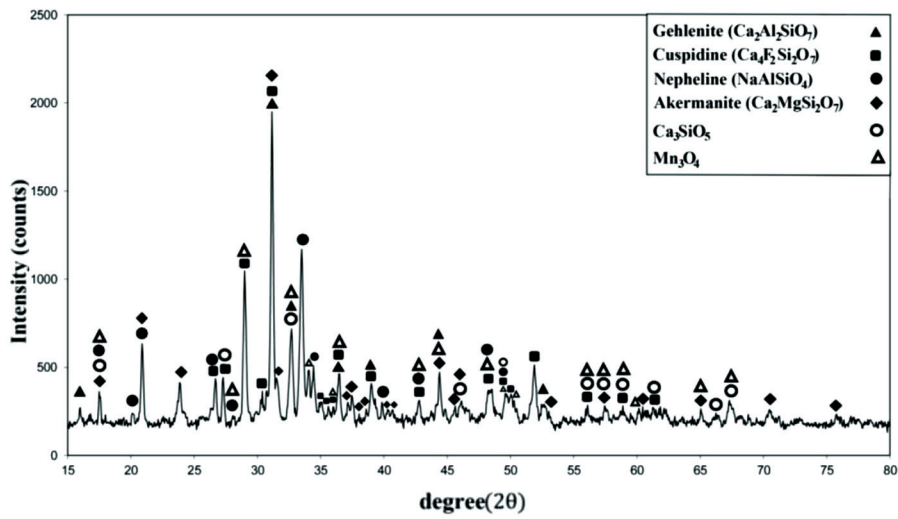


Fig. 10. XRD analysis of the sample C.

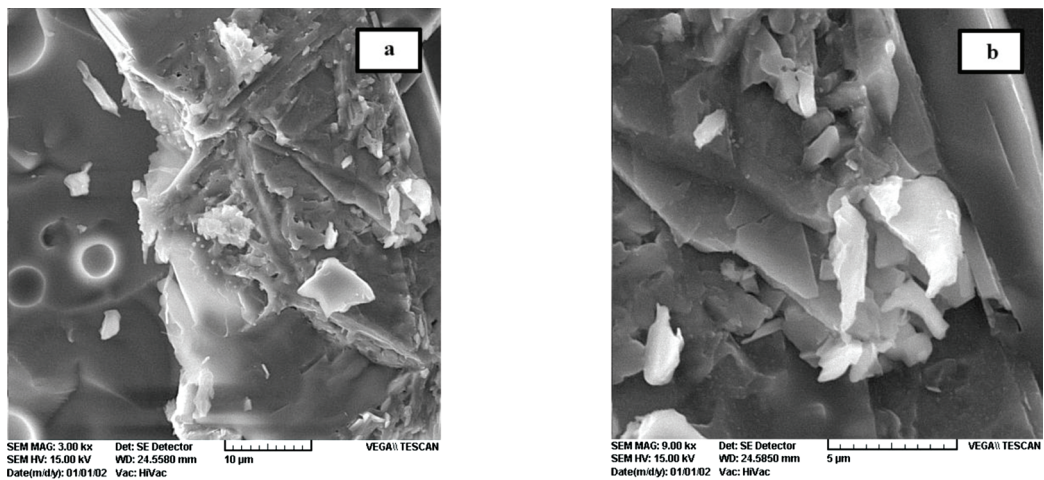


Fig. 11. SEM images of the sample C: (a) 3000x and (b) 9000x.

4. Conclusion

- Portland cement clinker can be used as the main compound to mold powder in continuous casting of steel.
- Hematite, zinc oxide, and sodium carbonate can be replaced a part of the fluorine in the mold powder composition and it can be consequently obtained a comparable viscosity relative to the viscosity of the reference sample.
- In the XRD analysis of the fired samples, gehlenite is the main phase with the most intense peak corresponding to the reference sample.
- In the XRD analysis of the molten samples, cuspidine, as a lubricating phase, was detected which can make crystalline sediment in the mold powder.
- It can be concluded that adding compounds such as zinc oxide and sodium carbonate to the mold powders, used in continuous casting of steel process, lead to obtain low-fluorine mold powders that it can be also led to the controlled viscosity and controlled horizontal heat transfer. As a result, these samples can be a suitable substitution for the main mold powder used in continuous casting of steel industry.

References

- [1] M. L. Koul, S. Sankaranarayanan, D. Apelian and W. L. McCaulery: *Mold powder Technology, Iron and steel Industry*, shenyang, PRC, (1988), 2.
- [2] A. B. Fox, K. C. Mills, D. Lever, C. Bezerra, C. Valadares, I. Unamuno, J.J. Laraudogoitia and J. Gisby: *ISIJ Int.*, 45 (2005), 1051.
- [3] J. A. Kromhout, S. Melzer, E. W. Zinngrebe, A. A. Kamperman and R. Boom: *Research int.*, 79 (2008), 51.
- [4] K. W. Yi, Y.T. Kim and D.Y. Kim: *metal. mater. Int.*, 13 (2007), 223.
- [5] H. J. Shin, S. H. Kim, B. G. Thomas, G. G. Lee, J. M. Park and J. sengupta: *ISIJ Int.*, 46 (2006), 1635.
- [6] K. C. Mills, A. B. Fox, R. P. Thackray and Z. Li: *ISIJ Int.*, 45 (2004), 722.
- [7] M. Hayashi, R. A. Abas and S. Seetharaman: *ISIJ Int.*, 44 (2004), 691.
- [8] G. Wen, S. Sridhar, P. Tang, X. QI and Y. Liu: *ISIJ Int.*, 47 (2007), 1117.
- [9] S.Y. Choi, D.H. Lee, D. W. Shin, S.Y. Choi, J. W. Cho and J. M. Park: *J.Non-cryst. solids*, 345-346 (2004), 157.
- [10] R.W. Soares, M.V.A. Fonseca, R. Neuman, V.J. Menezes, A.O. Lavinhas and J. Dweck: *Thermochim. Acta*, 318 (1998), 131.
- [11] M. C. C. Bezerra, C. A. G. Valadares, I. P. Rocha, J. R. Bolota, M. C. Carboni, I. L. de. Scripnic, C. R. Santos, K. Mills and D. Lever: *Steelmak, Seminar Int.*, Brazil, (2006), 10.
- [12] M. Hanao, M. Kawamoto and T. Watanabe: *ISIJ Int.*, 44 (2004), 827.
- [13] M. Hayashi, T. Watanabe, H. Nakada and K. Nagata: *ISIJ Int.*, 46 (2006), 1805.
- [14] M. Persson, M. Gornerup and S. Seetharaman: *ISIJ Int.*, 47 (2007), 1533.
- [15] K. Santhy, T. Sowmya and S. R. Sankaranarayanan: *ISIJ Int.*, 45 (2005), 1014.

The structure-property relationship in a desulfurised and degassing hot work W500 tool steel

M. Kalantar^{1*}, S.S. Ghasemi² and M.H. Saadati³

Department of Materials Engineering, Faculty of Mining and Metallurgy, Yazd University, Yazd, Iran

Abstract

The effect of secondary steelmaking processes such as desulphurization, removal of inclusions and vacuum degassing followed by hot forging and hardening heat treatment on the microstructure and mechanical properties of a hot-work w500 tool steel have been studied in details. In order to follow the progress of secondary steel making, the content of impurity elements such as S, P, O, H and N were measured. These elements influence the mechanical testing and the microstructure of the steel. The results show that desulfurization treatment can be accelerated at higher temperature of 1680 °C and 15 minutes holding time for silicon and aluminum with contents of 0.33% and 0.056% in the molten steel, respectively. In this condition, the removal percentage of sulfur has been reached to about 90% relative to the initial sulfur content. For the degassing sample A, the strength and the hardness, after hot working and quenching – tempering, have been increased from 976 to 2020 MPa and 29 to 52 R_c, respectively. Whereas for the normal sample B, the associated strength and the hardness have been changed from 870 to 1845 MPa and 21 to 55 R_c, respectively. The difference between mechanical properties of sample A and sample B can be related to the presence of Al₂O₃ clusters, silicate inclusions, and a longer filamentary inclusion in the microstructure of sample B after hot-forging. Microstructural observations show that the morphology of pearlite in the forged sample A is more uniform and carbide particles are also much finer than these particles in the non-degassing forged sample B.

Keywords: secondary steel making, hot work W500 tool steel, heat treatment, mechanical properties, microstructure.

1. Introduction

Hot work tool steels are a group of heat treatable carbon and alloy steels with high stability of hot and cold mechanical working properties¹⁻⁵. These types of steels, in general, are hypereutectoid ledburite containing carbides in the tempered martensitic matrix in which, hard carbide particles have been dispersed in the matrix in order to improve wear behavior of cold and hot working dies. The presence of strong carbide forming elements such as Cr, V, Nb, W and Mo along with high carbon content accelerate the formation of hard carbides in tool steels with a high hardness of 60-65 HRC. resulting a large fraction of the production cost for machining of dies⁶⁻⁷. Hot work tool steels are used for engineering applications including molds, punches, cutting and machining dies subjected to high thermal exposure as well as severe erosion conditions such as hot pressing, hot extrusion, hot forging, die casting and speed cutting tools⁸⁻⁹. These applications require high toughness, high resistance to thermo-

mechanical stresses, good resistance to erosion and thermal fatigue¹⁰⁻¹². Modern technology needs steels with a higher quality and the demands have been increased for steels with minimum inclusion, cavity, impurities such as phosphorous and sulfurous in which advanced physical and mechanical properties have been developed¹³⁻¹⁶. In this regard, the quality control of alloy steels has been improved by employing special techniques of secondary steelmaking treatments such as vacuum degassing, removing inclusion by blowing inert gas into the molten steel and deoxidizing by Al and Si with Ca-Si/Ca-Al agents. The purpose of this study is to investigate the effect of secondary steelmaking operations on the microstructure and mechanical properties of a developed hot work tool steel.

2. Materials and Experimental Methods

All experimental works related to the secondary steelmaking procedures were conducted in alloy steel company of Asfrayen. The samples of molten steel were taken from various stages of steel making process such as arc electric furnace, ladle furnace and vacuum degassers in different combination of melt chemical composition, holding temperature and time conditions. The chemical composition of the degassing (A) and the normal (B) steel samples were presented in Table 1.

* Corresponding author:

Tel: +98 (913)3513418, TeleFax: +98(351)8210995

Email: Mkalantar@yazduni.ac.ir

Address: Department of Materials Engineering, Faculty of Mining and Metallurgy, Yazd University, Yazd, Iran.

1,2. Associate Professor

3. Alloy Steel Company of Sfrayen

Table 1. The Chemical composition of degasified (A) and non-degasified (B) W500 tool steel samples

Sample	C _{eq}	C	Si	Mn	P	S	Cr	Mo	Ni	V
A	1.15	0.58	0.26	0.74	0.01	0.01	1.18	0.47	1.48	0.066
B	1.13	0.57	0.28	0.73	0.023	0.029	1.16	0.48	1.46	0.06

The samples A and B were hot-worked in order to modify the size and the morphology of columnar grains with non-uniform inclusions as well as to reduce casting porosity and voids. The hot working process was carried out by radial and edge hot working treatment in two stages as schematically illustrated in Fig. 1 and detailed in Table 2.

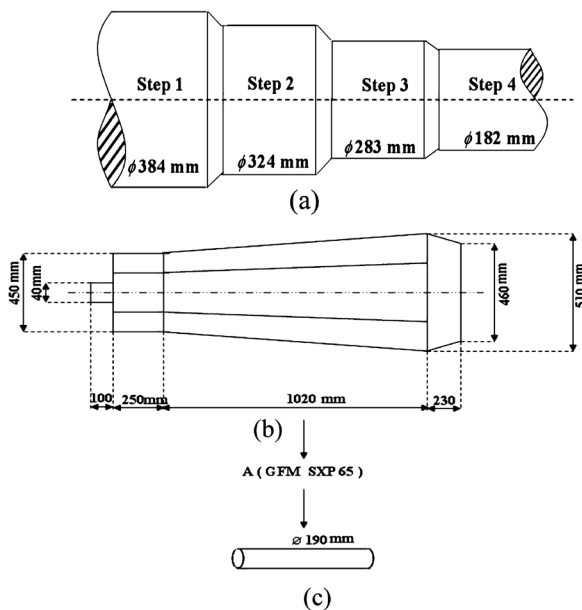


Fig. 1. The schematic representation of hot working process: (a) radial and edge hot-forging condition; (b) the initial sample; (c) the final hot-forged sample.

Table 2. Data related to Fig. 1(a).

Section	Diameter (mm)	Strain	RA%
1	384	0.71	51
2	324	1.05	65
3	283	1.35	74
4	182	2.23	84

A successive impact and homogeneous deformation were conducted during hot forging treatment. Before forging stage, the samples were homogenized according to the shown cycle of Fig. 2.

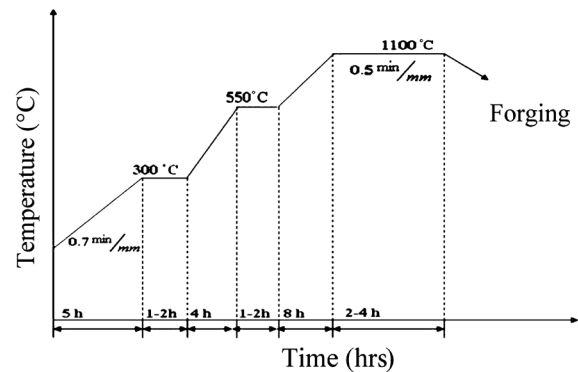


Fig. 2. The Heat treatment cycle of annealing before hot forging Stage.

The temperature of samples at the end of each forging stage should be at least 850 °C to avoid the formation of carbides continuously in grain boundaries. Because of low thermal conductivity, the hot forged samples were immediately placed in the annealing furnace to avoid initiate the thermal stress and micro-cracking on the subsequent cooling stage as shown schematically in Fig. 3.

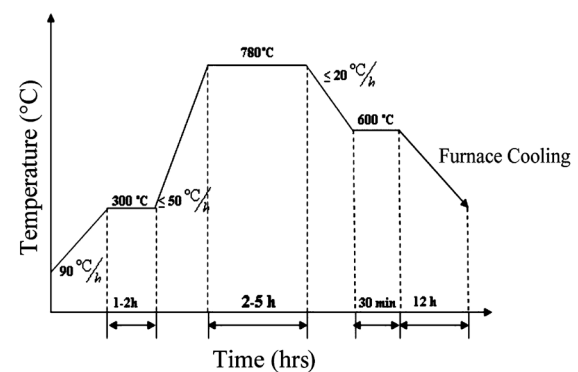


Fig. 3. The Heat treatment cycle of annealing after hot forging Stage.

Based on the chemical analysis given in Table 1 and the empirical following formula, the martensite start temperature (Ms) is about 233 °C. Therefore, a minimum temperature of 250 °C is necessary to decompose the retained austenite as shown in Fig. 4(b).

$$Ms (°C) = 512 - 453 C - 16/9 Ni + 15 Cr - 9.5 Mo + 217 (C)^2 - 71/5 (C)(Mn) - 67/6 (C)(Cr)$$

$$Ms (°C) = 512 - 453 \times (0.58) - 16/9 \times (1.48) + 15 \times (1.18) - 9.5 \times (0.47) + 217 \times (0.58)^2 - 71/5 \times (0.58) \times (0.74) - 67/6 \times (0.58) \times (1.18) = 233°C$$

Hardening heat treatment was performed on the austenized sample at the temperature of 850 °C by quenching in hot oil bath (Fig. 4a). In order to decompose the retained austenite completely and to improve the mechanical properties, a two-stage temper treatment was applied according to Fig. 4(b). The mechanical properties of samples A and B were determined after hot forging, annealing and heat treatments stages. Tension samples were prepared according to standard ASTM A 370 using a universal Zwick system. Impact samples were prepared according to standard ASTM E23. The microstructure of samples studied by optical microscopy. The amount of inclusions and cavities were measured according to standard DIN 50602 and ASTM E 45. All chemical compositions was analysed by a quantummetry instrument. The amount of impurity elements of sulfur, carbon, hydrogen, oxygen and nitrogen was determined by the equipment of model Leco, Ghlahp Selax and Hydrix.

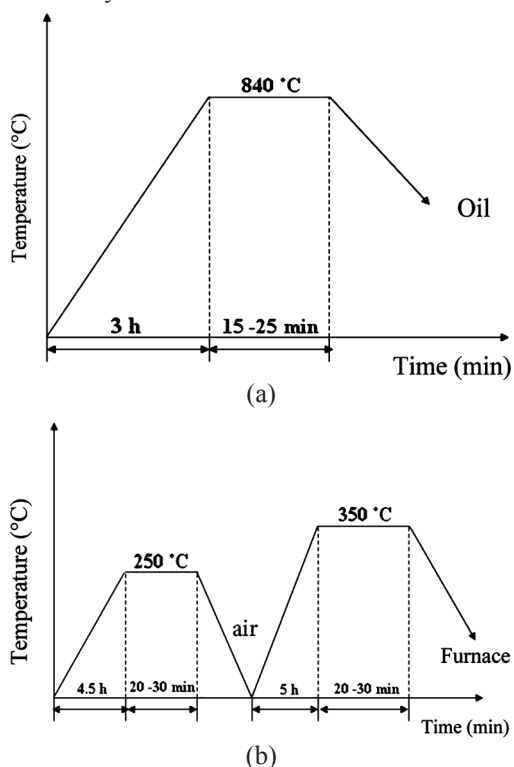


Fig. 4. Heat treatment cycles: (a) hardening; and (b) tempering treatments.

3. Results and Discussion

3.1. Secondary Steelmaking Process

In general, the desulfurization of molten steel can be facilitated by the presence of a basic slag including high content of CaO to minimize dissolved oxygen of the molten steel in making the ladle during secondary steel atmosphere at higher temperature. In order to decrease the solubility of oxygen, it is necessary to use strong oxide-forming elements such as Mn, Si, Al and Ca. In this investigation, with increasing of Al content

from 12 Kg to 28Kg per 50 tons of molten tool steel, removal percentage of the sulfur has been changed from 36% to 88% after VDP¹ treatment (Fig. 5) by the following reaction:



The use of higher content of Ca-Si agent in the molten steel leads to lower content of the sulfur as a consequence of direct reaction between calcium and sulfur (CaS), and indirect reaction between silicon and oxygen (SiO₂) respectively. For example, increasing Si content from 0.2% to 0.33%, the amount of the sulfur content remains still approximately 45% of the initial sulfur content (Fig. 6). With increasing the temperature of the molten steel from 1635°C to 1685°C at the beginning of VD processing, the residual amount of the sulfur in the molten steel is about 50% of the original one (Fig. 7), depending on the progress of the endothermic desulfurization reaction.

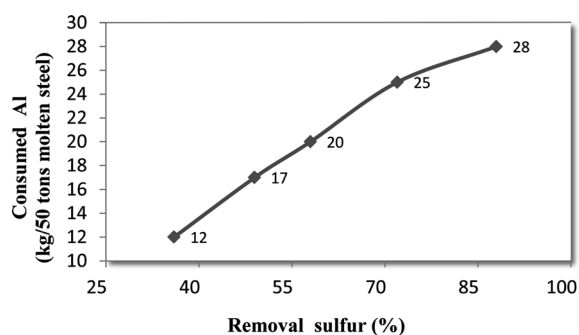


Fig. 5. The Effect of aluminum on the desulfurised treatment.

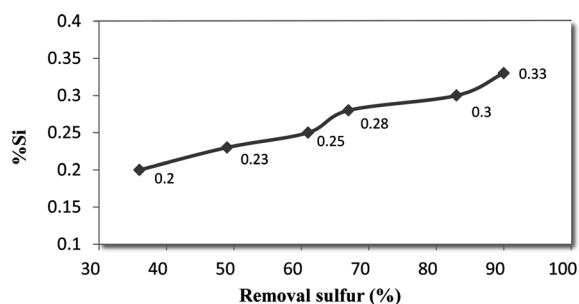


Fig. 6. The Effect of Si in the molten steel on the removal sulphur at 1635°C.

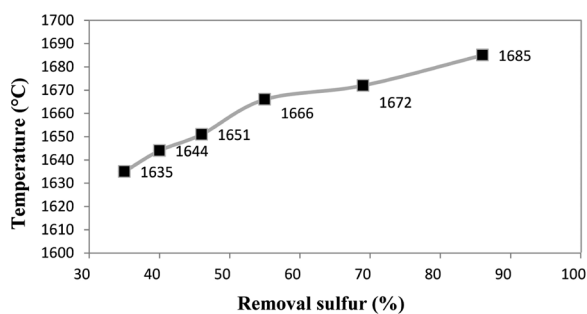


Fig. 7. The Effect of molten metal temperature on the removal sulfur.

¹ Vacuum Degassing Process

In the subsequent increase in holding time to more than 15 minutes at 1685 °C during VD processing, the amount of oxygen in the molten steel was increased along with the erosion and the solubility of refractory oxide lining, resulting a reduction in desulfurization rate (Fig. 8).

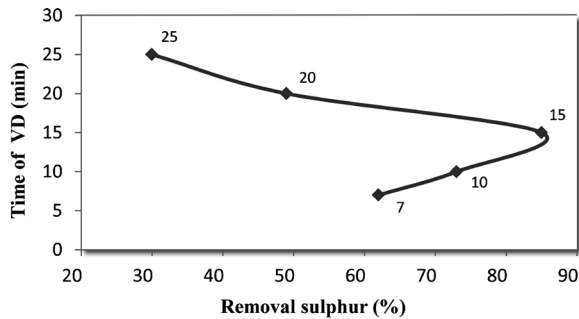


Fig. 8. The Effect of VD time on the desulfurisation at 1685 °C.

The amount of nitrogen in the sample B was determined about 71 ppm (Table 3) due to the formation of stable nitrides; whereas, this content for the degassed sample has been reached to 27.3 ppm. The solubility of oxygen in the molten steel in the electric arc furnace after the deoxidation stage is approximately 50 ppm which corresponding to oxygen content of the sample B (56 ppm in Table 3). For the degassed sample, the amount of soluble oxygen has been reached to 12.27 ppm. These observations are related to the mechanical properties developed in the samples A and B. As cleared in Table 4, there is a significant reduced value in tension strength and impact energy of the sample B in compared with the sample A. These results indicate that the mechanical properties of W500 tool steel is very sensitive to the solubility of hydrogen, oxygen and nitrogen. The presence of only 6.3 ppm soluble

hydrogen that is almost five times higher than soluble hydrogen content in degassed sample A (Table 3) could be more effective in the brittle fracture.

Table 3. The Content of soluble gases (H, O and N) in samples A and B.

Sample	ppm(H)	ppm(O)	ppm(N)
A	1.53	12.27	27.3
B	6.3	56	71

3.2. Mechanical Properties and Microstructures

In Table 4, mechanical properties of the sample A has been compared with the sample B after hot working, annealing, quenching, and tempering heat treatments. Obviously, the difference in mechanical properties of samples A and B are very high, so these observations can be related to differences in secondary steel making operations. For the degassing sample (A), because of the purification and removal of impurity elements such as sulfur and phosphorous, the level of inclusions and cavities have been decreased (Fig 9d). Consequently, the hot working operation is more effective in which a higher mechanical property has been developed in comparison with the forged sample B (Table 4). For the sample B, the clusters of Al_2O_3 and silicate inclusions can be formed as the long filamentary inclusions after hot-forging operation (Figs 9a,b,c) due to the low plasticity of inclusions; As a result, the micro-cracks can be initiated around these particles. Therefore, the derived results of tension strengths, hardness and impact toughness for the sample B are considerably less than these results for sample A (Table 4) which can be result of distributing non-uniform inclusions and blow-holes interaction in the matrix of tool steel.

Table 4. The mechanical properties of samples A and B after hot working, annealing, quenching and tempering heat treatments.

Condition	Tension Test				Impact test	Hardness test	Sample
	Ultimate Strength (MPa)	Yield Strength (MPa)	ϵ %	(A%)			
Hot working	976	878	16.6	31.54	39	29	A
	870.2	475.4	14	26	35	21	B
Annealing	1198	1080	14	19	32	24	A
	995	756	10	17.79	23	26	B
Quenching and Tempering	2026	1800	6.6	6.5	11	55	A
	1845	1720	5.9	5.7	9	52	B

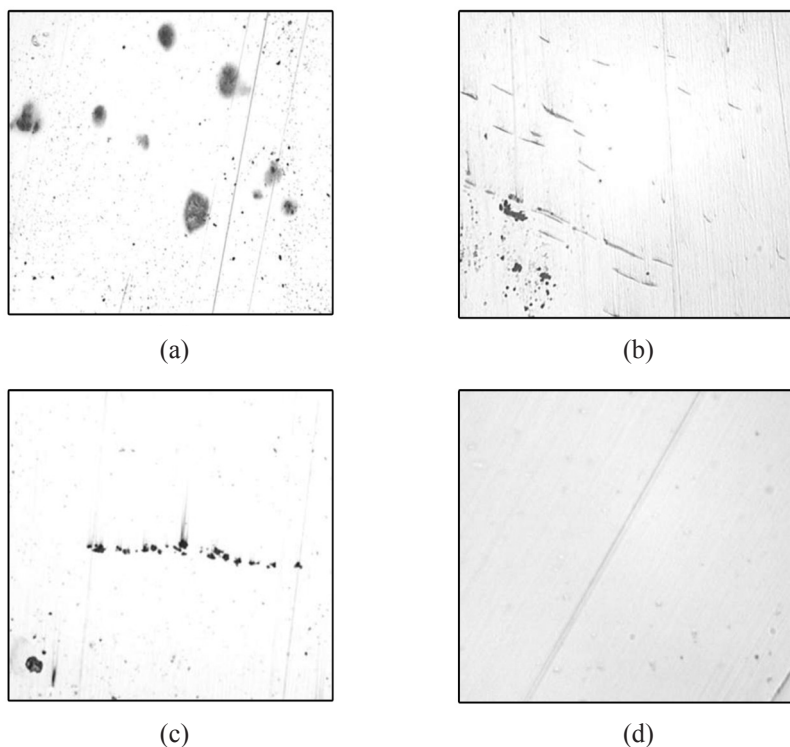


Fig. 9. The Optical microstructure of: (a, b, c) sample B; and (d) sample A (100X).

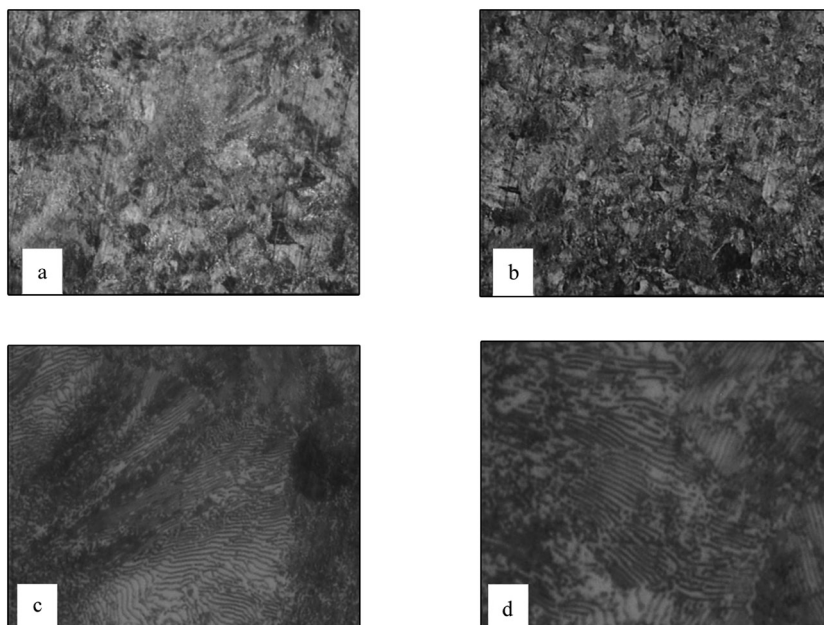


Fig. 10. The Optical microstructure after hot forging stage: (a) sample A (b) sample B (100X); (c) sample A; and (d) sample B (500 X).

The alumina inclusions can be converted to the calcium aluminates by adding Ca-Si agent to the molten steel, which reduce their negative effect on mechanical testing.

The microstructure of hot forged samples A and B are shown in Fig. 10. As is shown at higher magnifications in Figs. 10(c) and (d), there are fine Pearlite with the dispersed carbide particles in both microstructure of

samples A and B. It is obvious that the morphology of the pearlite in the hot-forged sample A is more uniform and carbide particles are much finer than these particles in the normal forged sample B.

Both hot-forged samples A and B after annealing give the more uniform microstructure in compared to the only hot-forged samples (Fig. 11).

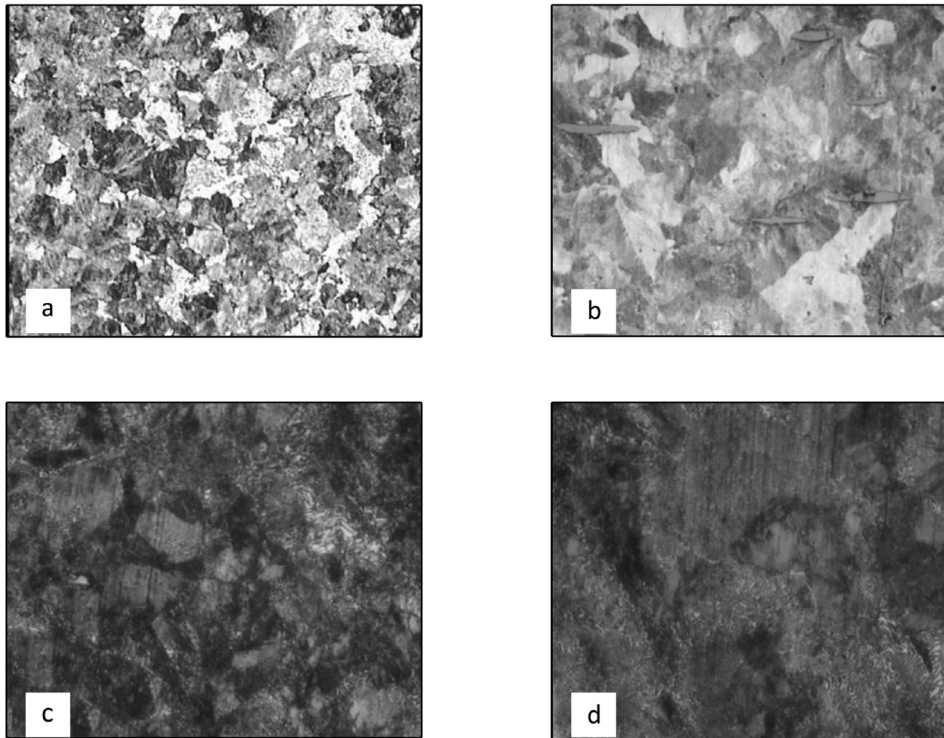


Fig. 11. The Optical microstructure after annealing treatment: (a) sample A; (b) sample B (100X); (c) sample A; and (d) sample B (500 X).

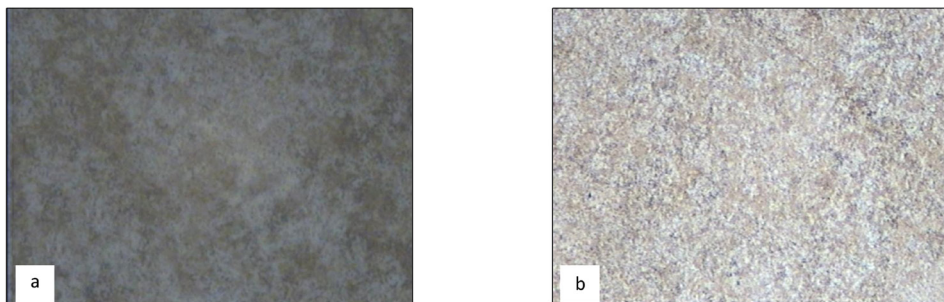


Fig. 12. The Optical microstructure after quenching and tempering Processes: (a) sample A; (b) sample B (500 X).

After quenching and tempering processes, it occurs the most difference between mechanical properties of samples A and B (Table 4). The formation of micro-crack around the inclusions in the sample B has been increased during the quenching stage as a consequence of interaction between hard martensitic structures and high solubility of hydrogen (6.3 ppm); so it reduces considerably mechanical properties in this sample. Also the high content of hydrogen (Table 3) is another reason which decreases mechanical properties of the sample B after hot forging, annealing, quenching and tempering treatments respectively. In the condition by higher hydrogen content than 6 ppm (the limited solubility), a hydride phase or a filamentary cavity can be formed in the microstructure which is more sensitive brittle behavior. It decreases impact toughness of steel (Table 4). The presence of

cavities and gas blows within the sample B can be lead to the reduction of the effective section size against the applied force; thus, stress concentration has been increased around the inclusions and so the localized stress initiates the formation and growth of micro-cracks during mechanical testing. As a result, necking phenomena in the sample B can be occurred at much less applied stress than the same one for the sample A (Table 4).

It has been formed fine martensite with carbide particles in the microstructure of both samples A and B after the quenching and tempering treatments (Fig. 12). Therefore, the tensile and yield strengths, hardness and impact energy of both samples, particularly the sample A, were significantly improved after quenching and tempering treatments compared to hot forging and annealing processes (Table 4).